

Design and Development of a Microscopic Electrical Impedance Tomography System

Abdulrahman Alfareh¹, Mohd Hafiz Fazalul Rahiman^{1*}, Masturah Tunnur Mohamad Talib¹, Khatijahusna Abd Rani², Ruzairi Abdul Rahim^{5,6}, Jaysuman Pusppanathan³, Fatin Aliah Phang⁴, Elmy Johana Mohd⁵

¹Tomography Imaging and Instrumentation Research Group, School of Mechatronic Engineering, Universiti Malaysia Perlis, Pauh Putra Campus, 02600 Arau, Perlis, Malaysia

²Institute of Engineering Mathematics, Universiti Malaysia Perlis, Pauh Putra Campus, 02600 Arau, Perlis, Malaysia

³Faculty of Biosciences and Medical Engineering, Universiti Teknologi Malaysia, 81310 UTM Johor Bahru, Johor, Malaysia

⁴Centre for Engineering Education (CEE), Universiti Teknologi Malaysia, 81310 UTM Johor Bahru, Johor, Malaysia

⁵Instrumentation and Sensing Technology Focus Group, Faculty of Electrical & Electronic Engineering, Universiti Tun Hussein Onn Malaysia (UTHM), Johor.

⁶Process Tomography Research Group (Protom-i), Faculty of Electrical Engineering, Universiti Teknologi Malaysia, 81310 UTM, skudai

Abstract: Basically, Electrical impedance tomography is a new technique in monitoring and imaging cross sectional images and physical state of objects by measuring the internal impedance distribution. This paper presents the design of a microscopic electrical impedance tomography system, which is a non-destructive approach that has the capability to interpret and analyze the internal impedance distribution of a medium (the system) and reconstruct its image as a tomogram, where any object inside the system can be shown in a 2D (two-dimension) image. A current source circuit was constructed and studied by injecting 5 mA of current to an array of electrodes (3*3 array). Moreover, the conditional measurement circuit is going to receive voltage from measurement electrodes array of 8*16 in each plane. The data was obtained from both planes as a matrix of 8*16 electrodes using multiplexers which was transferred serially to the PC to be analyzed and to reconstruct the image/tomogram. The image reconstruction process and algorithms were engaged in the calculation to reconstruct the image based on the voltage collected. Finally, interpolation is conducted to improve the quality and increase the resolution of the image.

Keywords: Renewable fuel, ethanol, numerical simulation, auto ignition, single-step mechanism

1.0 Introduction

With the rapid development and the revolution of technologies in science, materials and biotechnologies in the last decade. Electrical Impedance tomography (EIT) is seen to be playing a big role to improve and establish a modern approach of supervision and imagining physiological state of materials that depends on internal impedance distribution. The impedance of a conducting domain may include physical objects, tissue samples or human bodies. Currents are injected directly into the domain that resulting a current-voltage boundary [1]. Thus, the data acquisition is conducted sequentially with time and the data sets are measured to determine the values of transfer impedance, from which the internal impedance distribution is reconstructed as a cross-sectional image. Electrical characteristic imagining of diverse materials have been investigated for a few years in order to reconstruct or form the image of impedance

changes. The EIT is able to visualize the internal distribution of a conducting domain. Microscopic impedance imaging methods using conventional EIT techniques have been established in order to investigate the evolution and growing of cells during cultivation [13-16].

IET refers to the process of injecting current/voltage to a system and measuring the voltage/current in order to reconstruct a cross sectional image of an object [1]. EIT is one of the most important methods for imaging the distribution of electrical conductivity of an object. EIT has been effectively used in several applications since the 1960s. For instance, resistive components of the internal impedance is considered and estimated where this approach is called Electrical Resistance Tomography (ERT) which is applicable in geological applications [4]. However, when a reactive component of impedance is estimated, the approach is known as Electrical Capacitance Tomography (ECT).

Generally, the electrodes are used as connectors to measure voltages. The voltage measurement will be collected from receiving electrodes, where all the data is converted to the distribution of conductivity of an object, which is used to create a tomographic image by solving a regularized inverse model [2]. The advantage of this imaging system technique compared to the traditional imaging methods (PET, CT, MRI and ect.) is that it is non-invasive and non-distractive.

According to previous research, EIT has the potential to replace the conventional medical imaging techniques. Commonly, there are a few approaches of imaging techniques such as the following:

1. Computed Tomography (CT)
2. Mammography
3. Magnetic Resonance Imaging (MRI)
4. Positron Emission tomography (PET)
5. Ultrasound and Thermal imaging

Typical hardware of an EIT microscopic system has three major parts, which are EIT electrodes, electrical instruments, and a PC with reconstruction algorithm software. Electrodes are used to transmit the current inside the phantom / system from one to another. They also collect the observable signals that will be transferred to a measurement device. Electrical instruments are devices that are used to transmit and receive the measurement from the electrodes. Therefore, a current source circuit has been designed and built to transmit current through the electrodes. At the same time, a receiver circuit is designed to collect the voltage measurement and then the data is transferred serially to the PC for analysis and image reconstruction. Finally, the received analogue signals will be converted to digital via data conversion (ADC) to measure the boundary voltage potential. This basic block diagram as shown in Fig. 1.

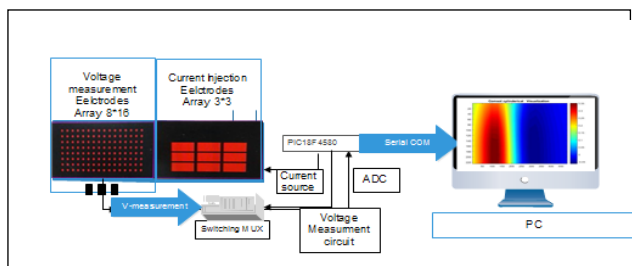


Fig. 1 System block diagram

2.0 Methodology

Comsol software is the virtual environment to build and investigate a system in order to compare the result with hardware outputs. Comsol design has been constructed to meet the specifications and fulfil the objectives of a system. Therefore, the design in Fig. 2.0 shows the two arrays of electrodes imaging planes to measure the voltage potential. At the other side is the current injection source array. Fig. 2.0 illustrates the full system, which has been implemented in Comsol software

design. Currents will be injected from current source array (source plane) to the sink plane tangentially with imaging planes. At the same time, the imaging planes will measure the voltage potential between both planes. This can be changed proportionally whenever the impedance of the system is changed. The sensor configuration of the sensor is shown in Fig. 2.

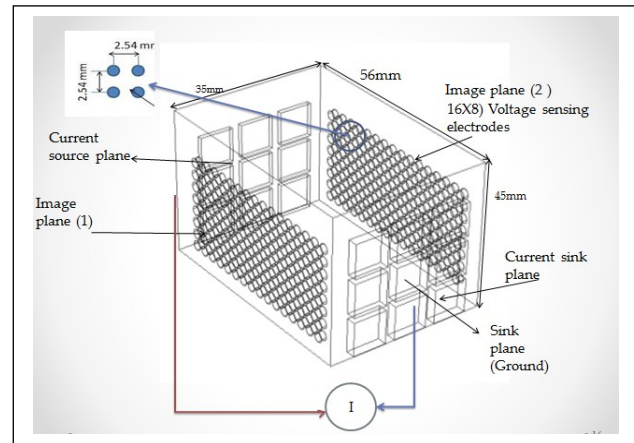


Fig. 2: System structure and design

2.1 Sensor Current Injection

In EIT, the current source is the essential part of EIT Microscopic. Many studies have been carried out using multiple constant current sources and alternative current sources to be excited through the electrodes [6]. In order to reconstruct the cross-sectional images, the measuring boundary voltage data is collected, processed and analyzed to obtain the image of the conductivity distribution. One of the limitations faced previously is the current source performance of the EIT system, where this factor determines the accuracy of the measurement. When several current sources are applied, calibration is very important to make the sum of all currents is always at zero. In this paper, we propose using multiple current sources to maximize the accuracy of the system and fast multi-channel voltmeters have been suggested in order to reduce the time of data acquisition. Usually, the current source consists of a voltage-to-current converter.

Therefore, we describe the design and implementation of the current source using LT3092 instrumentation amplifier. There are few approaches of injecting current used in previous designs such MarK1 Micro-EIT system and MarK2 [4-6]. One approach has been carried out in this project as shown in Fig. 4 which has the following features:

1. Injecting current from lower electrodes to upper current as positive terminal and lower current electrodes row at the other side as ground.
2. Injecting current from medium current electrodes (electrode number 5) as positive terminal and lower current electrodes at the other side as ground.

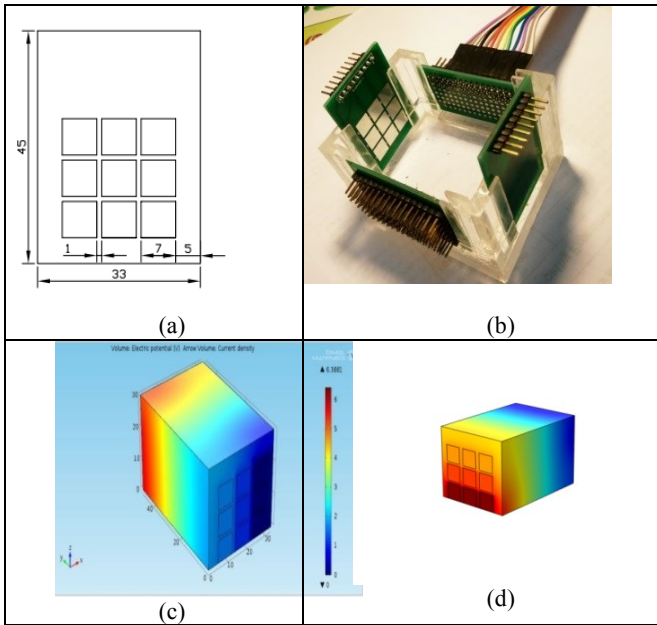


Fig. 4 (a) Current electrodes Dimensions in mm, (b) Hardware design structure , (c) 9 electrodes current injection , (d) lower row Current injection

Differential equations that governs the current flows in the medium is the Poisson’s Equation (1),

$$\nabla \cdot (\sigma \cdot \nabla U) = I \tag{1}$$

Where U is voltage, I is current and σ is the resistivity. It relates the dependency between conductivity distribution and the boundary voltages where the voltage is produced by injecting current across the object is governed by equation (2),

$$\nabla \cdot (\sigma + i\omega\epsilon) \nabla \phi = 0 \tag{2}$$

The sample σ is the electric impedance of the surrounding medium, ϕ is the electric potential, ω is the Frequency, and ϵ is the electric permittivity. Equation (1) is reduced to the standard. For injecting low frequency or direct current to the EIT system consequently, $\omega \approx 0$ [9].

3.0 Data Acquisition of voltage Measurement

There are four methods for voltage measurement, which are opposite approach, Trigonometric method, adjacent and cross method that has been applied in tomography and tangential approach. The tangential approach measurement has been used in this project to measure the voltage between the two planes. The project basic concept is to apply current through the current source to the electrodes inside the container and measure the voltage using differential voltmeters. The idea behind the differential voltage measurement is to measure the voltage between pairs of electrodes. Therefore, a voltmeter can be multiplexed to the PIC in order to measure continuously all the electrodes. The hardware implementation is a little complex. Thus, one of the project objectives is to minimize the complexity of the

hardware. The number of electrodes is an array consisting 16 columns and 8 rows of microscopic EIT system electrodes designed as shown in Fig. 5 using Altium circuit design software and fabricated as PCB.

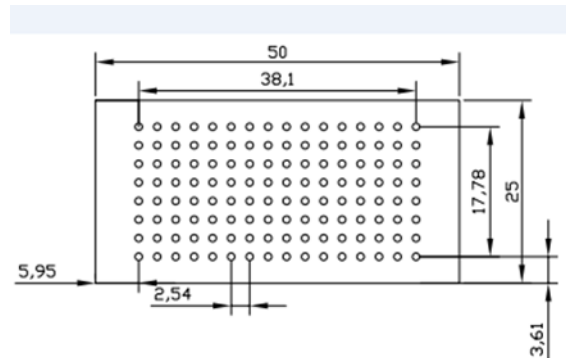


Fig. 5 Array of Receiving Electrodes in mm

The data transmission process collects data through a serial port communication between the controller and the PC. Here, MATLAB is used to interface with the microcontroller in order to arrange the measured value into a matrix form more easily.

4.0 Sensitivity map and Generation algorithm

There are three algorithms that could be applied in order to obtain the sensitivity map named as the following: Finite Element Method (FEM), Tikhonov regularization algorithm, Algorithms of Forward and inverse problems and the expectation maximization (EM) algorithm. These algorithms have been applied in tomography. Data has been obtained from the probes in both sides of the container (256 receivers) where the voltage potential between both sides is measured and the difference is calculated and normalized using equation (3). The percentage of average reading of the object is calculated as:

$$E = \frac{\text{Caliberated data} - \text{measurement data}}{\text{caliberated data}} \tag{3}$$

5.0 Result And Discussion

Data has been acquired from a Comsol design using boundary probes of a total number of 256 (128 for each plane) in order to obtain the precise voltage measurement. Laterally, the global variable definition has been created to get the voltage potential (average) between both planes. The data has been acquired and recorded to be sampled and analysed. The method that has been followed in this project is getting data from plane (1) and plane (2) which acts as reference points where the data is to be arranged as a matrix from both planes and sampled as showed in the data in Tables 1, 2, and 3.

Table 1: Calibrated Data (No Object)

1.024058	0.889914	0.764429	0.657066	0.574956	0.514904	0.478352	0.463565	0.469079	0.495238	0.54472	0.619077	0.720016	0.849883	1.010775	1.191466
1.049904	0.912798	0.784712	0.675272	0.588775	0.527555	0.4904	0.474537	0.480369	0.507219	0.559577	0.636142	0.739266	0.879946	1.039153	1.222445
1.066049	0.929552	0.800674	0.688284	0.601188	0.538712	0.499446	0.484773	0.489393	0.51653	0.570533	0.649558	0.755694	0.891486	1.058163	1.239867
1.073554	0.940875	0.810669	0.699227	0.609449	0.547534	0.507533	0.492397	0.496805	0.52708	0.579123	0.660376	0.766964	0.903609	1.069679	1.249405
1.081828	0.948006	0.818487	0.705418	0.615548	0.552921	0.513924	0.496642	0.503495	0.53206	0.585995	0.667146	0.775069	0.911313	1.07677	1.254376
1.08608	0.951901	0.822907	0.709666	0.620786	0.55825	0.518415	0.499543	0.505884	0.534934	0.59034	0.671485	0.778984	0.916977	1.081724	1.256449
1.089228	0.954927	0.823826	0.710786	0.623252	0.557014	0.518153	0.501314	0.506787	0.535058	0.591118	0.672483	0.781145	0.919894	1.084818	1.260545
1.095389	0.957123	0.823673	0.709732	0.620598	0.556039	0.515839	0.499436	0.505103	0.534761	0.588933	0.670869	0.78057	0.920367	1.088435	1.269757

Table 2: Measured Data (with object)

0.857401	0.71593	0.586728	0.488255	0.42928	0.408353	0.415265	0.437081	0.468934	0.509932	0.565502	0.640248	0.739807	0.866743	1.024886	1.201725
0.869822	0.721546	0.585759	0.482004	0.42181	0.407311	0.423436	0.452267	0.485911	0.538017	0.584513	0.661472	0.762078	0.891108	1.055174	1.235058
0.874621	0.721904	0.581046	0.472172	0.413344	0.404839	0.420269	0.464396	0.50079	0.544298	0.60096	0.678737	0.781641	0.913395	1.076356	1.255163
0.874873	0.720282	0.575453	0.466301	0.407186	0.402713	0.431071	0.471634	0.510756	0.556417	0.613054	0.692019	0.795302	0.928067	1.089951	1.266635
0.874204	0.718702	0.572892	0.462059	0.403842	0.400747	0.432391	0.474306	0.517334	0.562949	0.621922	0.701375	0.805483	0.937773	1.099179	1.273065
0.874995	0.718165	0.571456	0.461101	0.40341	0.399649	0.432685	0.474866	0.518828	0.565746	0.626522	0.706628	0.810396	0.944352	1.105033	1.276568
0.874731	0.720155	0.572413	0.461394	0.404202	0.398622	0.430258	0.473501	0.517672	0.565293	0.627417	0.708018	0.812982	0.947899	1.109064	1.281547
0.884963	0.723087	0.572985	0.461494	0.403446	0.397703	0.428357	0.470004	0.514505	0.563381	0.6251	0.706483	0.8125	0.948597	1.113325	1.291653

Table 3: Tomogram data of image

0.162742	0.195506	0.230462	0.256916	0.253369	0.206934	0.133385	0.057132	0.000308	-0.02967	-0.03815	-0.0342	-0.02649	-0.01984	-0.01396	-0.00861
0.170732	0.209533	0.253536	0.286154	0.283381	0.227926	0.136549	0.046911	-0.01154	-0.041	-0.04568	-0.03982	-0.03086	-0.02193	-0.01542	-0.01032
0.179568	0.223385	0.274304	0.311986	0.312456	0.248507	0.142512	0.042034	-0.02229	-0.04969	-0.05333	-0.04492	-0.03494	-0.02458	-0.01719	-0.01234
0.166888	0.234459	0.290179	0.333119	0.331867	0.264457	0.150654	0.042169	-0.02796	-0.05566	-0.05859	-0.04913	-0.03695	-0.02707	-0.01895	-0.01379
0.131913	0.241934	0.30006	0.344886	0.343332	0.275218	0.158648	0.044973	-0.02749	-0.05806	-0.06131	-0.05131	-0.03924	-0.02904	-0.02081	-0.0149
0.184355	0.245346	0.304718	0.350257	0.350163	0.281627	0.16537	0.049398	-0.02559	-0.0576	-0.06165	-0.05234	0.04002	-0.02985	-0.02155	-0.01601
0.194447	0.245354	0.305177	0.350889	0.351463	0.284359	0.16963	0.05549	-0.02148	-0.05651	-0.06141	-0.05284	-0.04076	-0.03044	-0.02235	-0.01666
0.193287	0.244521	0.304349	0.349762	0.349907	0.284757	0.173468	0.058358	-0.01861	-0.05352	-0.06143	-0.05309	-0.04091	-0.03067	-0.02287	-0.01724

4.1 Data Interpolation

Interpolation is a mathematical and statistical approach to estimate and construct new data between two known data values in sequence of values. During the measurement process that has been discussed before, we have found that some data has been taken with low accuracy and it is not easy to obtain. This implies that it is affected by an unknown contact impedance. Therefore, interpolation method is used to predict the missing values and to increase the resolution of the image. There are a few types of interpolation, which are cubic, cosine, linear and nearest, where the quality of the methods starts from the best to the worst. Fig. 6 (a), shows the object position and Fig. 6 (b) is the Tomogram without Interpolation. After the tomogram image visualization is being interpolated, the image is clearer and can be easily recognized as shown in the Fig. 7.

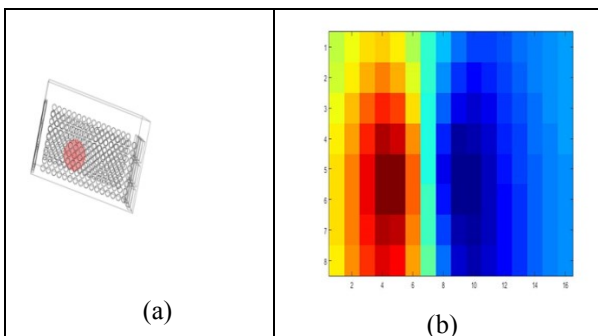


Fig. 6 Tomogram without Interpolation

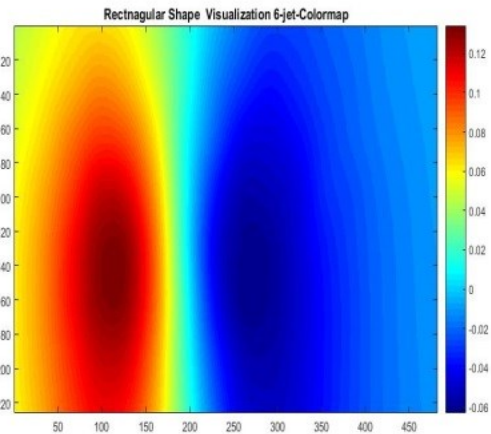


Fig. 7 Tomogram image with Interpolation

One example is provided to show the importance of interpolation as shown Fig. 8. By comparing both results in Fig. 8 (a) and Fig. 8 (b), the shape of the object can be clearly recognized. Fig. 8.0(a) is the sample system in 3D while Fig. 8 (b) is the side view of the system to show the position of the object. Interpolation result in Fig. 8 (d) is the visualization with interpolation, which has the clearer image of the sphere object in high intensity of impedance.

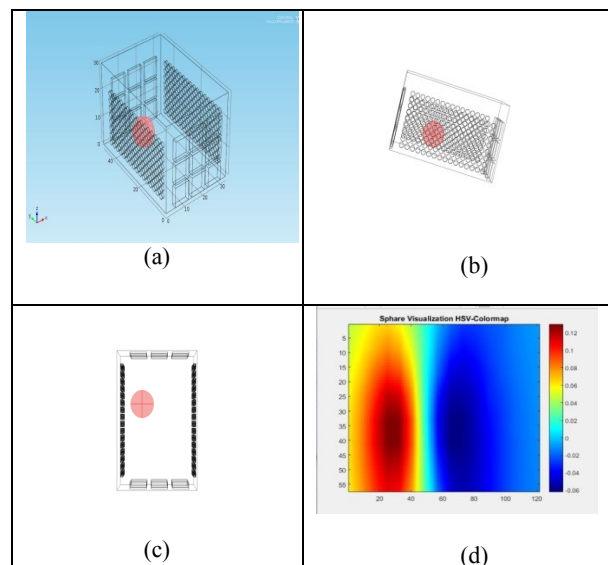


Fig. 8 Sphere object Visualization

When we put a sphere object of an acrylic plastic, the image (Tomogram) where the sensor loose error applied to get full and precise image shows the internal impedance distribution.

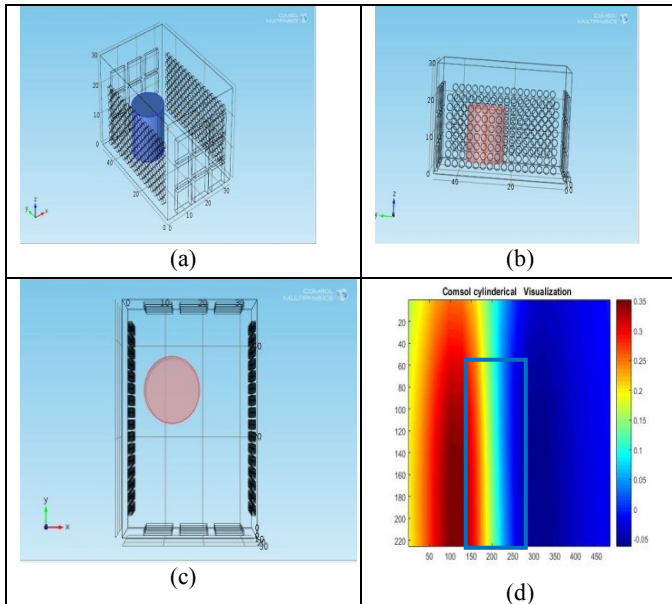


Fig. 9 Cylindrical Shape Visualization

Impedance, which illustrates the sensor loose error in this area, is high and the resistivity of the current flow increased based on the object that acted as resistance inside the container. Both images have been obtained by the same color map and interpolation. We have investigated two shapes with different sizes to prove the ability of the system:

1. A sphere shape which has a radius of 7 mm, placed near to the injecting corner as shown in Fig. 8 (b), position near to the corner in Fig. 8 (a) from different views in 3D, and the image tomogram in Fig. 8.0(d).
2. A cylindrical shape has been designed and tested to be included in this investigation, to fulfill the objectives of the project. The cylindrical size is 3mm radius, with 10mm height. Fig. 9 (a) with a 3D view shows the dimensions of the cylindrical shape. The image in Fig. 9 (d) shows the shape, size and position of the object after image reconstruction.

6.0 Conclusion

Referring to the experiment, the measurement voltages of each electrode have been collected and tabled as matrixes for each plane. The data have been transferred into tomograms. Tables 3 shows the value of voltage of a potential difference between the planes (plane 1 and plane 2) of the Comsol simulation and hardware. The data is then further processed by a set of MATLAB image reconstruction algorithm to visualise the internal impedance and conductivity. Based on images in Fig. 7, it can be easily observed that each of the tomogram for different shapes has the same characteristics as the original shape. Colours of the object has been put between two planes and measuring the voltage potential.

For example, red colour in the image implies the high impedance of the object position. Thus, it indicates that different position of object can be recognized and detected by using this approach. The colour intensity of a tomogram represents the conductivity distribution of the object. It is scaled from dark red to dark blue. Dark red means high resistivity, while dark blue indicates low resistivity. From the experiment, the system has been tested. With different colour intensity, we are able to inspect and recognise the shape, size of the object. Finally, the sensitivity of the tomogram may be also affected by the complexity of the system, due to number of electrodes. It would indirectly lead to poor connectivity and hence influence the final result which leads to low resolution of the image. The final reconstructed image will be subjected to noise.

References

- [1] T. K. Bera, "Sensors for Electrical Impedance Tomography."
- [2] T. Naidoo, "Signal and Image Processing for Electrical Resistance tomography."
- [3] F. R. M. Yunus, R. A. Rahim, S. R. Aw, N. M. N. Ayob, M. P. Jayasuman, and M. F. Jumaah, "Front-End Circuit in Electrical Resistance Tomography (ERT) for Two-Phase Liquid and Gas Imaging," *J. Teknol.*, vol. 70, no. 3, Sep. 2014.
- [4] A. Report, "AN-1515 A Comprehensive Study of the Howland Current Pump," no. April, pp. 1–17, 2013.
- [5] F. Application and P. Data, "5,919,142," vol. 15, 1999.
- [6] D. G. April, "Choose resistors to minimize errors in grounded-load current source," vol. 43, no. 3, pp. 2009–2011, 2013.
- [7] P. Bertemes-filho, A. Felipe, and V. C. Vincence, "High Accurate Howland Current Source: Output Constraints Analysis," vol. 2013, no. November, pp. 451–458, 2013.
- [8] P. Bertemes-filho, V. C. Vincence, M. M. Santos, and I. X. Zanatta, "Low power current sources for bioimpedance measurements: a comparison between Howland and OTA-based CMOS circuits," vol. 3, no. 41, pp. 66–73, 2012.
- [9] M. Cheney and D. Isaacson, "Issues in Electrical Impedance Imaging," pp. 53–62, 1995.
- [10] M. Cheney, D. Isaacson, and J. C. Newell, "Electrical Impedance Tomography *," vol. 41, no. 1, pp. 85–101, 1999.
- [11] R. D. Cook, G. J. Saulnier, D. G. Gisser, J. C. Goble, J. C. Newell, and D. Isaacson, "ACT3: A High-speed, High-Precision Electrical Impedance Tomograph," vol. 41, no. 8, pp. 713–722, 1994.
- [12] Z. Cuil, H. Wang, L. Tang, L. Zhang, X. Chen, and Y. Yan, "A Specific Data Acquisition Scheme for Electrical Tomography," no. c, pp. 3–6, 2008.
- [13] P. P. Data, "(12) Ulllited States Patent Tanaka," vol. 2, no. 12, 2013.
- [14] D. Garg, "Design and development of Electrical Impedance Tomography (EIT) based System," vol. 74, no. 7, 2013.
- [15] M. Goharian, "New Hardware and Software Design for Electrical Impedance Tomography," 2007.
- [16] D. S. Holder, "ELECTRICAL IMPEDANCE Edited by," 2005.
- [17] N. T. Holliday, "EIT DATA PROCESSING SYSTEM AND," vol. 2, no. 12, 2011.
- [18] H. Hong, "Comparison of a new integrated current source with the modified Howland circuit for EIT applications," vol. 999.
- [19] K. Karhunen, A. Seppänen, A. Lehtikoinen, P. J. M. Monteiro, and J. P. Kaipio, "Cement and Concrete Research Electrical Resistance Tomography imaging of concrete," *Cem. Concr. Res.*, vol. 40, no. 1, pp. 137–145, 2010.